

Synthesis and Structure of LaSr₂CuTiO_{6.5}: A New Oxygen-Deficient Ruddlesden–Popper Phase

Gregory M. Sarjeant, Kevin B. Greenwood, and Kenneth R. Poeppelmeier*

Department of Chemistry and the Science and Technology Center for Superconductivity,
Northwestern University, 2145 Sheridan Road, Evanston, Illinois 60208-3113

Hong Zhang, Paul A. Salvador, Thomas O. Mason, and Laurence D. Marks

Department of Materials Science and Engineering and the Science and Technology Center for
Superconductivity, 2137 Sheridan Road, Evanston, Illinois 60208-3108

Received May 14, 1996[⊗]

The structure of LaSr₂CuTiO_{6.5}, a novel (ABO₃)_nAO *n* = 2 Ruddlesden–Popper phase, has been solved by powder X-ray diffraction and electron microscopy. The diffraction patterns are consistent with *I4/mmm* symmetry, with tetragonal lattice parameters *a* = 3.8816(1) Å and *c* = 20.296(2) Å. The structure of LaSr₂CuTiO_{6.5} is similar to Sr₃Ti₂O₇, with copper and titanium disordered over the single B-cation site, and lanthanum and strontium almost perfectly disordered over the two A-cation sites. The oxygen content, determined by thermogravimetric reduction to be 6.5 (±0.1), is consistent with divalent copper with the oxygen vacancies distributed within the perovskite layers. The absence of local order and strategies for inducing a layered arrangement of the B-cations are discussed.

Introduction

Since the discovery of superconductivity in La_{2-x}Ba_xCuO₄ in 1986,¹ intense exploratory research has yielded a large number of materials containing CuO₂ planes interleaved by spacer layers, insulating blocks, and charge reservoirs. This wealth of compounds is an essential aid in determining how the structure and defect chemistry of materials affect their high-temperature superconducting behavior. Notwithstanding this history of preparatory success, novel compounds continue to be synthesized, and many opportunities to prepare layered cuprates (as well as other transition-metal oxides) with interesting compositions, structures, and physical properties remain. In particular, the potential for new materials can be demonstrated in the system of perovskite-like oxides containing copper and titanium; however, the chemical factors which control the layering are only partially understood.

Owing to the size similarities between Cu²⁺ (Jahn–Teller radius ≈ 0.60 Å)² and Ti⁴⁺ (0.605 Å),³ BO_{4/2} (B = Cu or Ti) nets derived from either of these cations exhibit similar lattice dimensions. Thus these nets (or 2-D planes) can be incorporated into materials with either a complete segregation of both B-cations to separate layers (having minimal mismatch between such layers), or with a statistical distribution of the two B-cations within a single layer. The former arrangement leads to materials with the structural requirements for high-*T_c* superconductivity, and this structural motif is exhibited in the quadruple perovskites,

Ln'Ln''Ba₂Cu₂Ti₂O₁₁ (Ln = lanthanide, Y),^{4–10} which contain double sheets of corner-sharing copper–oxygen square pyramids that are separated by double sheets of corner-sharing titanium–oxygen octahedra. The difference between the coordination environments of copper and titanium in the quadruple perovskites is the driving force behind the cation order. Similarly, Gd₂CaBa₂Cu₂Ti₂O₁₂ is composed of double CuO₅ pyramidal sheets interleaved by two TiO₆ octahedral block layers and an additional (Gd,Ca)O rock salt layer.¹¹ Also, the structures of Gd_{2.33}Ce_{0.67}Ba₂Cu₂Ti₂O_y and Gd_{2.4}Ce_{0.6}Ba₃Cu₂Ti₃O_y are proposed to contain double layers of CuO₅ square pyramids separated by multiple TiO₆ octahedra layers and (Gd,Ce)O fluorite layers.¹² Despite the occurrence of distinct CuO_{4/2}²⁻ layers in the aforementioned compounds, doping studies have not yet realized superconductivity in these materials. Examples where copper and titanium do not order into individual layers include La₂CuTiO₆^{13–16} and La₂Ba₂Cu₂Ti₂O₁₁.^{8,17} In these materials, a variety of chemical

(4) Gormezano, A.; Weller, M. T. *J. Mater. Chem.* **1993**, 3(7), 771.

(5) Gormezano, A.; Weller, M. T. *J. Mater. Chem.* **1993**, 3(9), 979.

(6) Greenwood, K. B.; Anderson, M. T.; Poeppelmeier, K. R.; Novikov, D. L.; Freeman, A. J.; Dabrowski, B.; Gramsch, S. A.; Burdett, J. K. *Physica C* **1994**, 235–240, 349.

(7) Palacín, M. R.; Fuertes, A.; Casañ-Pastor, N.; Gómez-Romero, P. *Adv. Mater.* **1994**, 6(1), 54.

(8) Gómez-Romero, P.; Palacín, M. R.; Rodríguez-Carvajal, J. *Chem. Mater.* **1994**, 6(11), 2118.

(9) Greenwood, K. B.; Sarjeant, G. M.; Poeppelmeier, K. R.; Salvador, P. A.; Mason, T. O.; Dabrowski, B.; Rogacki, K.; Chen, Z. *Chem. Mater.* **1995**, 7(7), 1355.

(10) Palacín, M. R.; Krumeich, F.; Caldés, M. T.; Gómez-Romero, P. *J. Solid State Chem.* **1995**, 117, 213.

(11) Fukuoka, A.; Adachi, S.; Sugano, T.; Wu, X.-J.; Yamauchi, H. *Physica C* **1994**, 231, 372.

(12) Li, R. *J. Mater. Chem.* **1994**, 4(5), 773.

(13) Anderson, M. T.; Greenwood, K. B.; Taylor, G. A.; Poeppelmeier, K. R. *Prog. Solid State Chem.* **1993**, 22, 197.

(14) Palacín, M. R.; Bassas, J.; Rodríguez-Carvajal, J.; Fuertes, A.; Casañ-Pastor, N.; Gómez-Romero, P. *Mater. Res. Bull.* **1994**, 29(9), 973.

(15) Gómez-Romero, P.; Palacín, M. R.; Casañ, N.; Fuertes, A.; Martínez, B. *Solid State Ionics* **1993**, 63–65, 603.

[⊗] Abstract published in *Advance ACS Abstracts*, September 1, 1996.

(1) Bednorz, J. G.; Müller, K. A. *Z. Phys. B* **1986**, 64, 189.

(2) The Cu²⁺ ionic radius value corresponds to the equatorial radius for a distorted Jahn–Teller copper ion. This value was estimated from a survey of bond lengths given for several layered cuprates. The value differs from that given by Shannon because the equatorial bonds tend to be smaller than the apical bonds; therefore the average value does not reflect the anisotropic nature of this cation.

(3) Shannon, R. D. *Acta Crystallogr.* **1976**, A32, 751.

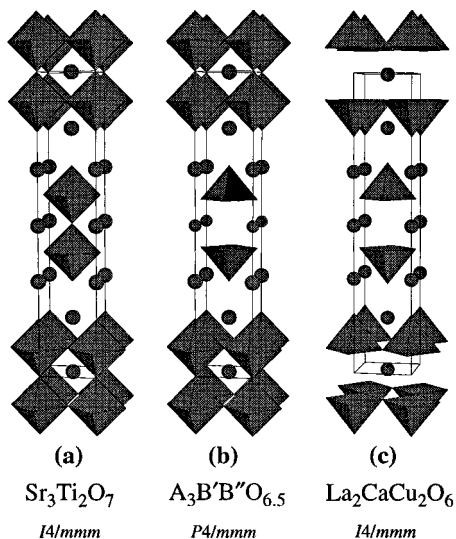


Figure 1. Structures of $n = 2$ Ruddlesden–Popper phases: (a) $\text{Sr}_3\text{Ti}_2\text{O}_7$, (b) an idealized oxygen-deficient phase with a layered arrangement of the B-cations, and (c) the oxygen-deficient material $\text{La}_2\text{CaCu}_2\text{O}_6$.

factors (such as overall oxygen stoichiometry, A-cation sizes, and coordination preferences of the B-cations) favor a distribution of the similarly sized Cu^{2+} and Ti^{4+} cations within a single $\text{BO}_{4/2}$ layer. Although the chemical factors which determine the B-cation order in perovskites containing copper and titanium have been discussed with relation to the above compounds, new materials offer the opportunity to explore these factors more fully as well as to yield interesting physical properties. The goal of the present study is to further our understanding of the cation ordering in highly oxygen-deficient materials, which in the above compounds favors layered (ordered) structures and potential candidates for superconductivity.

Ruddlesden and Popper have described a family of perovskite intergrowth structures with the general formula $\text{A}_{n+1}\text{B}_n\text{O}_{3n+1}$, where n is the number of ABO_3 perovskite layers separated by an individual AO rock salt layer.¹⁸ For example, $\text{Sr}_3\text{Ti}_2\text{O}_7$, depicted in Figure 1a, is an $n = 2$ Ruddlesden–Popper phase with every two SrTiO_3 perovskite layers (having Ti^{4+} in octahedral coordination) separated by an SrO rock salt layer.¹⁹ An oxygen-deficient analogue of the $n = 2$ Ruddlesden–Popper structure is illustrated in Figure 1c and has the nominal stoichiometry $\text{La}_2\text{CaCu}_2\text{O}_6$.²⁰ This structure can be derived from the former $\text{Sr}_3\text{Ti}_2\text{O}_7$ structure by replacing titanium with copper, strontium with lanthanum and calcium, and removing the oxygen atoms between the planes of copper atoms. Copper adopts square-pyramidal coordination in this material, and the overall oxygen content is lowered from seven to six, referenced from the titanate compound, owing to the different charge states on the constituent cations. In the representation shown, all of the calcium is located in the plane of the ordered oxygen vacancies. This

compound, which contains distinct $\text{CuO}_{4/2}$ nets, can be made to superconduct at 60 K.²¹ It is straightforward to envision an $n = 2$ Ruddlesden–Popper phase which contains the structural elements of both $\text{Sr}_3\text{Ti}_2\text{O}_7$ and $\text{La}_2\text{CaCu}_2\text{O}_6$, as shown in Figure 1b. This model can be derived from the $\text{Sr}_3\text{Ti}_2\text{O}_7$ structure by replacing only half of the Ti^{4+} with Cu^{2+} and choosing A-cations such that a nominal oxygen content of 6.5 is achieved (by consideration of charge neutrality). Because of the preference of Ti^{4+} for octahedral coordination and the stability of Cu^{2+} in square-pyramidal coordination, the oxygen vacancies may order to allow distinct layers of copper pyramids and titanium octahedra as shown in Figure 1b. One example of a material with the proper stoichiometry to potentially achieve this structure is $\text{LaSr}_2\text{CuTiO}_{6.5}$, of which the synthesis and structure are reported in the present investigation.

Experimental Section

Synthesis. $\text{LaSr}_2\text{CuTiO}_{6.5}$ was synthesized by a solid-state reaction technique. Stoichiometric amounts of high-purity ($\geq 99.99\%$) La_2O_3 , SrCO_3 , CuO , and TiO_2 were used as starting materials. The La_2O_3 was heated at 600 °C for 1 h prior to convert any hydroxide back into the oxide, and SrCO_3 was annealed in CO_2 at 800 °C to remove hydroxide and nitrate impurities. The starting materials were ball-milled for 25 min, placed in an alumina boat, and fired for 14 days at 975 °C with several intermediate regrindings.

X-ray Diffraction. Powder X-ray diffraction data were collected on a Rigaku diffractometer with Ni filtered $\text{Cu K}\alpha$ radiation from 10 to 90° 2θ with a step size of 0.05° and a counting time of 20 s. Silicon was used as an internal standard. The lattice parameters and structure of $\text{LaSr}_2\text{CuTiO}_{6.5}$ were refined using Rietveld analysis.²² Profiles of diffraction patterns based on ordered and disordered models of the B-cations were also calculated using the program LAZY to calculate the effects of cation ordering on the relative intensities of the diffraction peaks.²³

Transmission and High-Resolution Electron Microscopy. Transmission electron microscopy (TEM) samples were prepared by crushing $\text{LaSr}_2\text{CuTiO}_{6.5}$ powdered samples in anhydrous methanol and subsequently dispersing them onto clean 1000 mesh copper grids. High-resolution electron microscopy (HREM) images and electron diffraction patterns (EDPs) were taken using a Hitachi H9000 microscope operated at 300 kV. HREM images and EDPs were digitized to 8 bits using an Optronics P1000 microdensitometer and analyzed with Semper 6 software. That the local stoichiometry (of the grains from which the HREM images and EDP's were taken) corresponded to the overall nominal stoichiometry was confirmed with X-ray energy dispersive spectroscopy (system from EDAX) using a Philips CM30 operated at 300 kV.

Thermogravimetric Analysis. Hydrogen reduction thermogravimetry was performed using a Dupont Instruments 951 thermogravimetric analyzer. Approximately 50 mg powder samples of $\text{LaSr}_2\text{CuTiO}_{6.5\pm 0}$ were heated to 800 °C in a 7% H_2 /93% N_2 atmosphere until an equilibrium weight was established. The reduction products were identified by an X-ray diffraction trace, and the measured weight loss was used to calculate the overall oxygen content.

Results

Single-phase material was obtained after the preparation described above, and the powder X-ray diffraction

(16) Palacin, M. R.; Bassas, J.; Rodríguez-Carvajal, J.; Gómez-Romero, P. *J. Mater. Chem.* **1993**, *3*(11), 1171.

(17) Salvador, P. A.; Shen, L.; Mason, T. O.; Greenwood, K. B.; Poeppelmeier, K. R. *J. Solid State Chem.* **1995**, *119*, 80.

(18) Ruddlesden, S. N.; Popper, P. *Acta Crystallogr.* **1958**, *11*, 54.

(19) Elcombe, M. M.; Kisi, E. H.; Hawkins, K. D.; White, T. J.; Goodman, P.; Matheson, S. *Acta Crystallogr. B*, **1991**, *47*, 305.

(20) Kinoshita, K.; Izumi, F.; Yamada, T.; Asano, H. *Phys. Rev. B* **1992**, *45*(10), 5558.

(21) Cava, R. J.; Batlogg, B.; van Dover, R. B.; Krajewski, J. J.; Waszczak, J. V.; Fleming, R. M.; Peck, W. F., Jr.; Rupp, L. W., Jr.; Marsh, P.; James, A. C. W. P.; Schneemeyer, L. F. *Nature* **1990**, *345*, 602.

(22) Wiles, D. B.; Sakthivel, A.; Young, R. *Rietveld Analysis Program, Version DBWS-9006*, School of Physics, Georgia Institute of Technology, 1990.

(23) Yvon, K.; Jeitschko, W.; Parthe, E. *LAZY Pulverix*, Laboratoire de Crystallographie aux Rayons-x, Université de Genève, 1977.

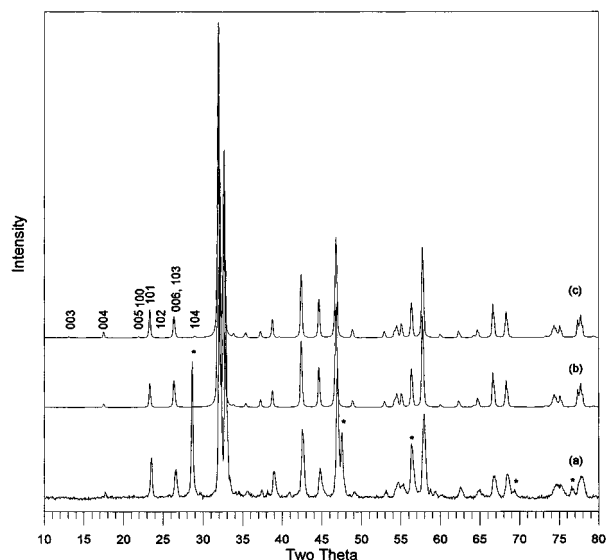
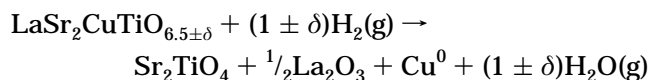


Figure 2. X-ray diffraction patterns of (a) $\text{LaSr}_2\text{CuTiO}_{6.5}$ obtained experimentally (silicon internal standard reflections marked by asterisks), (b) $\text{LaSr}_2\text{CuTiO}_{6.5}$ calculated using the atomic positions of $\text{Sr}_3\text{Ti}_2\text{O}_7$ with disordered B-cations and oxygen vacancies in the $I4/mmm$ space group, (c) $\text{LaSr}_2\text{CuTiO}_{6.5}$ calculated using the atomic positions of $\text{Sr}_3\text{Ti}_2\text{O}_7$ with ordered B cations and oxygen vacancies in the $P4/mmm$ space group.

pattern of this material is shown in Figure 2a. Reduction of the single-phase material at 800°C occurred via the following reaction:



The oxygen content was determined to be 6.5 ± 0.1 , which is consistent with divalent copper and that 1/14 (or 0.5/7) of the total oxygen sites are vacant.

The reflections of the X-ray diffraction pattern of the polycrystalline $\text{LaSr}_2\text{CuTiO}_{6.5}$ sample, shown in Figure 2a, could be indexed on a tetragonal cell with the dimensions $3.88 \times 3.88 \times 20.3 \text{ \AA}$. A few weak peaks (those near 41, 58.5, 59.3, and 38.3 2θ) could not be indexed on this cell or any related cells and are attributed to a small fraction of impurity phases that cannot be ascertained from these data. The diffraction pattern was similar to that of the Ruddlesden–Popper phase $\text{Sr}_3\text{Ti}_2\text{O}_7$ ($I4/mmm$ symmetry) with only the $h + k + l = 2n$ reflections appearing.¹⁸ In $\text{Sr}_3\text{Ti}_2\text{O}_7$, the Ti cations occupy a six-coordinate site and the oxygen sites are fully occupied. However, in $\text{LaSr}_2\text{CuTiO}_{6.5}$ the oxygen stoichiometry is not sufficient to provide octahedral coordination about all of the B sites. The oxygen vacancy is expected in the coordination sphere of copper, as Cu^{2+} can adopt coordination numbers less than six while the highly charged Ti^{4+} strongly prefers an octahedral coordination environment. If CuO_5 square pyramids and TiO_6 octahedra were disordered over the single B site, then the $I4/mmm$ symmetry would be retained, as observed in the PXD data. However, if the B–O polyhedra were ordered in the layered fashion illustrated in Figure 1b, the body-centering translation would be removed and the symmetry would be reduced to $P4/mmm$ (neglecting further structural distortions; for examples, see Elcombe et al.¹⁹), and the reflections $h + k + l = 2n + 1$ would appear.

To understand how cation and oxygen ordering affects the intensities of diffracted peaks in the $\text{LaSr}_2\text{CuTiO}_{6.5}$ system, the powder diffraction patterns of structures based on the $I4/mmm$ and $P4/mmm$ symmetries were first calculated using the program LAZY²² and the atomic positions for $\text{Sr}_3\text{Ti}_2\text{O}_7$.¹⁹ In the $I4/mmm$ model, the copper, titanium, and oxygen vacancies were completely mixed over their respective sites, while in the $P4/mmm$ model the B cations and oxygen vacancies were ordered in distinct layers. A complete mixture of the lanthanum and strontium over the A-cation sites was employed in both models as this produced calculated patterns that most closely resembled the pattern obtained experimentally. The resulting patterns are depicted in Figure 2. The observance of $h + k + l = 2n + 1$ reflections would provide evidence for ordering; however, as seen in the $P4/mmm$ pattern of Figure 2c, these reflections are extremely weak owing to the similar scattering capabilities of copper and titanium and the weak scattering ability of oxygen. These odd reflections are not observed in the experimental data but would be difficult to discern owing to their weak intensities which are on the order of signal-to-noise detectability. Moreover, Rietveld refinements of the structure in both the $I4/mmm$ and the $P4/mmm$ space group yielded similar values for the goodness of fit, indicating that X-ray diffraction was ineffective at determining the cation ordering unambiguously. Therefore, electron microscopy was implemented to determine the proper space group and cation arrangement.

Figure 3 shows the electron diffraction patterns along the [001] (a) and [100] (b) directions of the $\text{LaSr}_2\text{CuTiO}_{6.5}$ structure. All of the observed reflections could be indexed using the $3.88 \times 3.88 \times 20.3 \text{ \AA}$ tetragonal cell found from the X-ray diffraction data. Reflections indicative of an expanded unit cell (i.e., a superstructure resulting from possible complex ordering patterns of the cations and/or oxygen vacancies) were not observed, and only reflections satisfying an $h + k + l = 2n$ condition were present. This extinction condition is consistent with a body-centered structure of $I4/mmm$ symmetry. None of the EDPs or HREM images collected on different grains provided evidence that copper and titanium were locally ordering, and the sample appeared homogeneous by these electron diffraction investigations. In addition, compositional analysis using EDS on multiple grains evidenced that the local cation stoichiometry was that of the nominal stoichiometry (within the experimental error of several atomic percent), further supporting the mixed B-cation arrangement. Figure 4 is the corresponding HREM images to the EDPs in Figure 3 along both the [001] (a) and the [100] (b) directions. A centered unit cell (corresponding to an $n = 2$ Ruddlesden–Popper structure) is apparent in the HREM image along the [100] direction as shown in Figure 4b.

The structure of $\text{LaSr}_2\text{CuTiO}_{6.5}$ was thus refined by Rietveld analysis in $I4/mmm$ symmetry using the atomic positions of $\text{Sr}_3\text{Ti}_2\text{O}_7$ as a starting model.¹⁸ Copper and titanium were disordered over the $4e$ B-cation site, while the occupancies of lanthanum and strontium were refined over the two A-cation sites. The total occupancy of the A cations was constrained to maintain a 1:2 ratio of La:Sr. In the initial refinements, the oxygen vacancies were constrained to the O(1) site, which is between the adjacent B–O planes, and the O(2) and O(3) sites

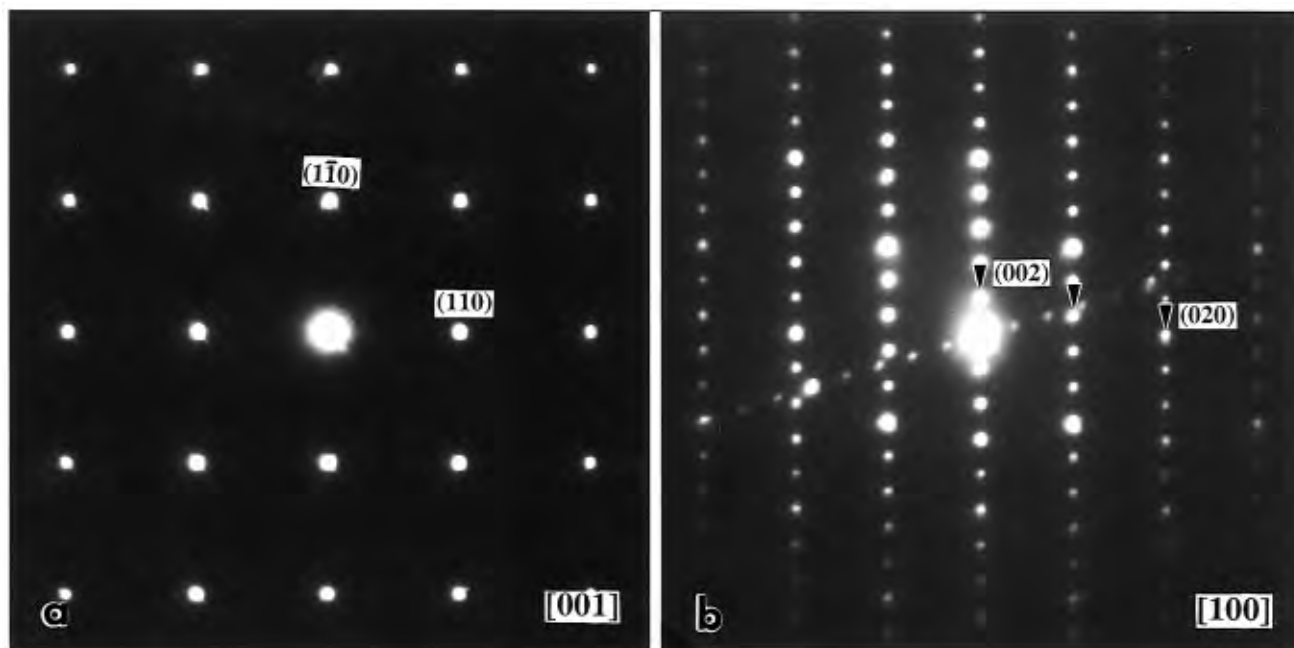


Figure 3. Electron diffraction patterns of $\text{LaSr}_2\text{CuTiO}_{6.5}$ taken along the (a) [001] and (b) [100] directions. The diagonal series of reflections in (b) result from diffraction along the [100] of a neighboring grain.

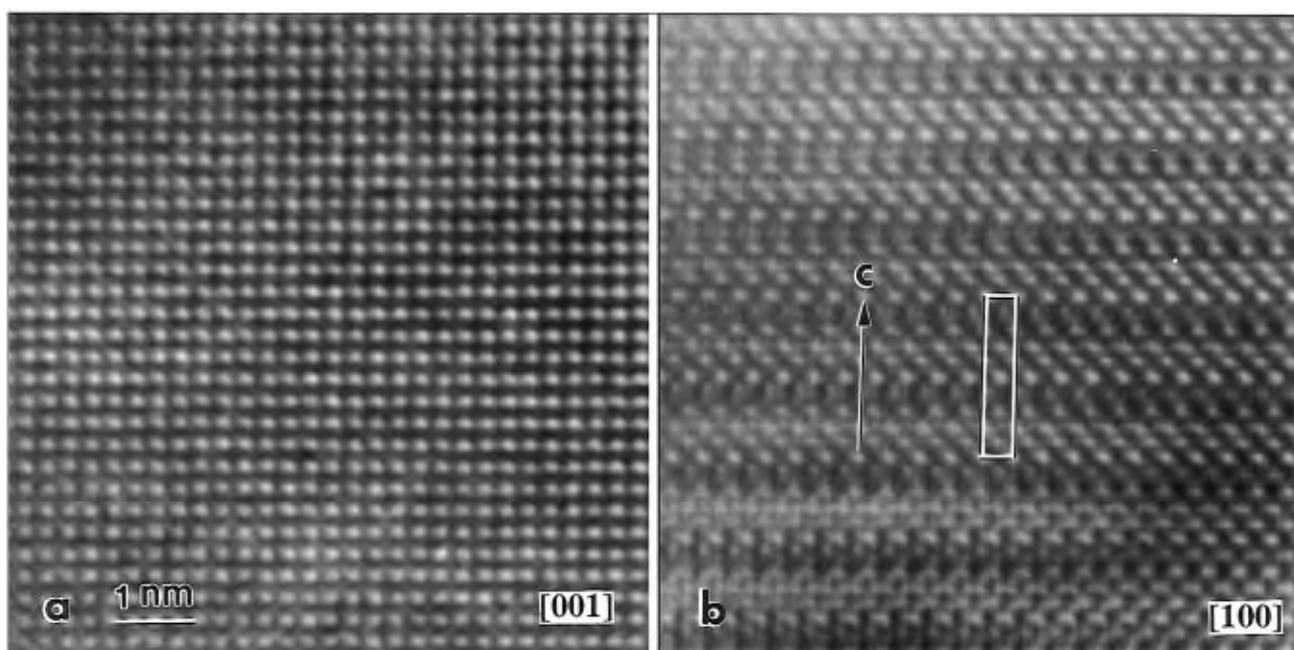


Figure 4. Experimental high-resolution electron microscopy images of $\text{LaSr}_2\text{CuTiO}_{6.5}$ taken along the (a) [001] and (b) [100] directions. A centered cell is outlined in Figure 4b.

were fully occupied. To maintain the correct overall oxygen stoichiometry, the O(1) site was only half-occupied. Using this model, a good fit was achieved between the calculated and observed intensities, and reasonable values were obtained for all crystallographic parameters except the thermal parameters of the oxygen.

The above-described model resulted in a negative thermal parameter for the O(1) site, indicating that this site has a larger occupancy than 50%. Therefore a variety of models with different vacancy distributions were tested, all of which had little effect on any of the crystallographic parameters except the thermal parameters and occupancies of the oxygen sites. As expected, owing to the weak X-ray scattering capability of oxygen,

the various oxygen vacancy models were indistinguishable based on the refinement statistics, and correlations between the occupancies and thermal parameters hindered an unambiguous determination of the location of the oxygen vacancies. After testing a variety of models, however, it became evident that, while there is a distribution of the vacancies over the oxygen sites in this structure, the vacancies are heavily concentrated on the O(1) site. Because of the inability of X-ray powder diffraction to resolve the distribution of oxygen vacancies, a vacancy model (described below) which yielded reasonable thermal parameters and occupancies of the oxygen sites and was consistent with known crystal chemical principles (see Discussion), was selected. Neutron diffraction experiments are currently

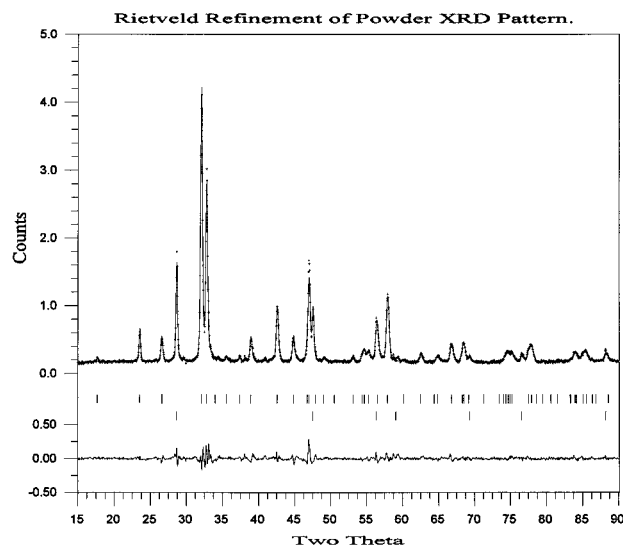


Figure 5. Experimental (dotted line) and calculated (solid line) X-ray diffraction pattern of $\text{LaSr}_2\text{CuTiO}_{6.5}$. Small bars indicate the positions of Bragg reflections for $\text{LaSr}_2\text{CuTiO}_{6.5}$ (upper bars) and silicon (lower bars). The difference between the calculated and experimental patterns is plotted along the bottom.

Table 1. Refined Structural Parameters for $\text{LaSr}_2\text{CuTiO}_{6.5}$ (Space Group No. 139, $I4/mmm$, $a = 3.8816(1)$ Å, $c = 20.296(2)$ Å)^a

atom	site	x	y	z	β (Å ²)	occup
A1	2b	0.5	0.5	0	0.70(22)	0.38(3) La/0.62(3) Sr
A2	4e	0.5	0.5	0.1816(1)	0.25(13)	0.31(3) La/0.69(3) Sr
B	4e	0	0	0.0959(3)	0.15(13)	0.5 Cu/0.5 Ti
O(1)	2a	0	0	0	1	0.700(9)
O(2)	8g	0	0.5	0.0906(9)	1	0.950(9)
O(3)	4e	0	0	0.1995(12)	2.02(58)	1

^a $R_p = 5.98$, $R_{wp} = 7.69$ where $R_p = 100(\sum |Y_{obs} - Y_{calc}| / \sum Y_{obs})$; $R_{wp} = 100\sqrt{(\sum W(Y_{obs} - Y_{calc})^2 / \sum W Y_{obs}^2)}$, where $W = 1/Y_{obs}$. Y_{obs} and Y_{calc} are the observed and calculated profile intensities at a given 2θ angle.

Table 2. Bond Lengths (Å) and Angles (deg) for $\text{LaSr}_2\text{CuTiO}_{6.5}$

atoms	bond lengths	atoms	bond angles
A1–O(1)	4 × 2.75		
A1–O(2)	8 × 2.67		
A2–O(3)	4 × 2.77	A(2)–O(3)–A(2)	165
	1 × 2.41		
A2–O(2)	4 × 2.68		
B–O(1)	1 × 1.95		
B–O(2)	4 × 1.94	B–O(2)–B	174
B–O(3)	1 × 2.10		

being conducted to more accurately determine the distribution of oxygen vacancies in this structure.

The oxygen vacancies in the final model were constrained within the perovskite blocks, which are the O(1) and O(2) sites. For these two sites, the thermal parameters were fixed to stable values found during the initial stages of the refinement, and the occupancies were allowed to vary such that the overall stoichiometry was maintained at 6.5. The occupancy of the O(3) site was constrained to be fully occupied while the thermal parameter was refined. This model led to reasonable and stable values for all parameters. Figure 5 illustrates the final profile fit and the difference pattern from the Rietveld analysis. The lattice parameters of $\text{LaSr}_2\text{CuTiO}_{6.5}$ were refined to $a = 3.8816(1)$ Å and $c = 20.296(2)$ Å. Crystallographic data and bond lengths

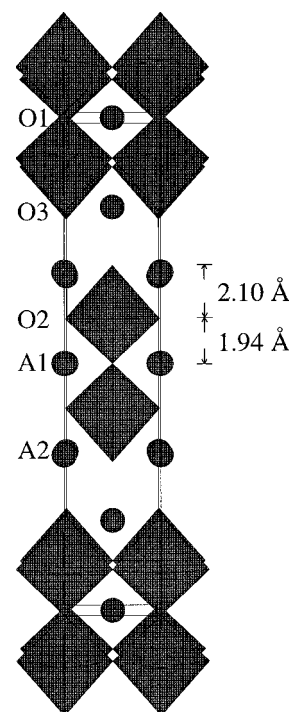


Figure 6. Structure of $\text{LaSr}_2\text{CuTiO}_{6.5}$. Oxygen vacancies are not shown.

and angles are given in Tables 1 and 2, respectively, and the structure is illustrated in Figure 6.

Discussion

The structure of $\text{LaSr}_2\text{CuTiO}_{6.5}$ has been determined from powder X-ray diffraction and electron microscopy and can be described as an oxygen-deficient member of the $n = 2$ Ruddlesden–Popper series. The most striking chemical feature is that copper and titanium are disordered over a single crystallographic site, despite the large number of oxygen vacancies in the coordination sphere of copper. In the known oxygen-deficient perovskite compounds containing copper and titanium, as well as the intergrowths of these phases with rock salt and fluorite blocks, long-range order is generally observed for copper and titanium. This ordering occurs to preserve the octahedral environment of Ti^{4+} , while Cu^{2+} adopts a Jahn–Teller distorted square-pyramidal environment. However, mixing of these polyhedra within layers has been observed in $\text{La}_2\text{Ba}_2\text{Cu}_2\text{Ti}_2\text{O}_{11}$ as determined by X-ray, neutron, and electron diffraction.^{7,8,17} Short-range order in $\text{La}_2\text{Ba}_2\text{Cu}_2\text{Ti}_2\text{O}_{11}$ was evidenced by electron diffraction owing to the observation of intensity at peaks corresponding to the layered quadruple perovskite structure in the EDPs.⁷ In the present investigation, however, no evidence of either long- or short-range order was observed, and copper and titanium are distributed randomly over a single site in $\text{LaSr}_2\text{CuTiO}_{6.5}$. In contrast to the other known oxygen-deficient mixed copper–titanates, mentioned above, the occurrence of oxygen vacancies in combination with different coordination preferences of the multiple B-cations does not result in a layered structure for $\text{LaSr}_2\text{CuTiO}_{6.5}$.

The statistical distribution of copper and titanium in $\text{LaSr}_2\text{CuTiO}_{6.5}$ resembles that of $\text{La}_2\text{CuTiO}_6$, an oxygen stoichiometric perovskite which has no driving force for the segregation of copper and titanium to distinct

polyhedra (as it contains only octahedra).^{13–16} A similar distribution of cations has also been observed in the compound LaSr₂CuRuO_{7–δ}, which is isostructural with LaSr₂CuTiO_{6.5} but has a much lower concentration of oxygen vacancies and pentavalent ruthenium as the second B-cation.²⁴ In the copper–ruthenium compound, there is no driving force for order based on coordination preferences of the multiple B-cations, unlike the oxygen-deficient copper titanates. Despite the random cationic distribution in LaSr₂CuTiO_{6.5}, which is consistent with that observed in related materials, there is yet potential to induce ordering by chemical substitutions on the A-site in this structure (see below).

The location of the oxygen vacancies in LaSr₂CuTiO_{6.5} could not be quantitatively determined in the current work. We propose that they are distributed over the O(1) and O(2) sites in the perovskite layer, with a higher concentration on the O(1) site. In known oxygen-deficient Ruddlesden–Popper cuprate materials^{25–31} (as well as other transition-metal materials^{24,32–34}) vacancies are typically located on the O(1) and O(2) sites, which supports our hypothesis on the location of the vacancies in LaSr₂CuTiO_{6.5}. Chemical arguments based on bond lengths and coordination preferences of the cations also support this model. The BO₆ octahedra in LaSr₂CuTiO_{6.5} are elongated along the crystallographic *c* axis (perpendicular the BO_{4/2} planes). This distortion is most noticeable in the B–O(3) bond length which is approximately 0.15 Å greater than either the B–O(1) or B–O(2) distances (see Table 2). This elongation is consistent with both the two-dimensionality of the Ruddlesden–Popper structure and a Jahn–Teller distortion of the Cu²⁺ cations. Although the B–O(1) and B–O(2) bond lengths (see Table 2) are nearly identical, the anisotropic distortion of the BO₆ octahedra effectively favors the occurrence of vacancies at the O(1) site rather than the O(2) site. The large difference between the B–O(1) and the B–O(3) bond distances, both of which are along the same axis of the octahedra, provides for a stabilization, although not a complete stabilization, of the vacancies at the O(1) site.

In the *I4/mmm* Ruddlesden–Popper structure there are two A-cation sites: a *2b* site that is 12 coordinate when all of the oxygen positions are fully occupied as in Sr₃Ti₂O₇, or 8 coordinate when oxygen vacancies concertedly order as in La₂CaCu₂O₆, and a *4e* site that is nominally 9 coordinate. Because of the size similarities between La³⁺ and Sr²⁺ (1.36 vs 1.44 Å, respectively, 12-coordinate radii)³ these cations mix substantially

over both sites in the structure. In LaSr₂CuTiO_{6.5}, the fully occupied *2b* and *4e* sites are approximately 38% and 31% occupied by La, respectively, where a 33% occupation factor on both sites would describe perfect disorder of the lanthanum and strontium. This distribution is similar to that observed in related materials^{24,29,35} and also has implications on both the oxygen vacancy and B-cation order. While mixing occurs for lanthanum and strontium in the known Ruddlesden–Popper phases based on copper, preferential site occupancy (8 coordinate, *2b* site) has been observed for calcium and yttrium cations.^{20,36–41} The site selectivity and preference for 8-fold coordination of yttrium and calcium may lead to concerted oxygen vacancy and B-cation order in substituted derivatives of LaSr₂CuTiO_{6.5}.

The oxygen-deficient Ruddlesden–Popper cuprate materials are known to have variable oxygen contents dependent on the size of the A-cation separating the copper–oxygen planes. The strontium-containing phases, La_{2–x}Sr_{1+x}Cu₂O_{6±δ}, intercalate oxygen when annealed in oxidizing environments, resulting in an increase in the distance separating CuO_{4/2} planes as δ increases and the ability to exceed an oxygen content of 6.0.^{29,36,42} However, when calcium occupies the site between the copper–oxygen planes, as in La₂CaCu₂O_{6±δ}, an oxygen content of 6.0 cannot be exceeded, and the *c* axis (perpendicular to the CuO_{4/2} planes) does not vary within detectable limits over the range of accessible δ values, suggesting that oxygen does not intercalate into the vacant oxygen sites between the CuO_{4/2} sheets.^{20,36,37,43} Moreover, Ruddlesden–Popper phases with more complex defect structures are known to occur among oxygen nonstoichiometric materials,²⁵ such as NdSr₂Cu₂O_{5.76},³¹ in which the high oxygen vacancy concentration is limited to sites similar to the O(1) and O(2) sites in LaSr₂CuTiO_{6.5}. Extending these ideas to a multiple B-site material, oxygen intercalation between CuO_{4/2} nets creates a driving force for mixing of the two B cations. A-site cations, such as lanthanum and strontium, which allow for such disorder on the oxygen sublattice therefore can stabilize a random distribution of two B-cations, as in LaSr₂CuTiO_{6.5}.

Transitions in the arrangements of the B cations and oxygen vacancies have been observed in perovskite-like materials as a function of A-cation composition.⁴⁴ For example, the aforementioned quadruple perovskite La₂Ba₂Cu₂Ti₂O₁₁ contains a disordered arrangement of the B-cations,^{8,17} whereas in the related compounds

(24) Atfield, M. P.; Battle, P. D.; Bollen, S. K.; Kim, S. H.; Powell, A. V.; Workman, M. J. *Solid State Chem.* **1992**, *96*, 344.

(25) Nguyen, N.; Choisnet, J.; Raveau, B. *Mater. Res. Bull.* **1982**, *17*, 567.

(26) Grasmeyer, J. R.; Weller, M. T. *J. Solid State Chem.* **1990**, *85*, 88.

(27) Caignaert, V.; Retoux, R.; Hervieu, M.; Michel, C.; Raveau, B. *J. Solid State Chem.* **1991**, *91*, 41.

(28) De Leeuw, D. M.; Mutsaers, C. A. H. A.; Geelen, G. P. J.; Langereis, C. J. *Solid State Chem.* **1989**, *80*, 276.

(29) Caignaert, V.; Nguyen, N.; Raveau, B. *Mater. Res. Bull.* **1990**, *25*, 199.

(30) Currie, D. B.; Weller, M. T.; Rowles, S.; Gregory, D. H. *Mater. Res. Bull.* **1990**, *25*, 1279.

(31) Caignaert, V.; Retoux, R.; Michel, C.; Hervieu, M.; Raveau, B. *Physica C* **1990**, *167*, 483.

(32) Poeppelmeier, K. R.; Leonowicz, M. E.; Longo, J. M. *J. Solid State Chem.* **1982**, *44*, 89.

(33) Dann, S.; Weller, M. T.; Currie, D. B. *J. Solid State Chem.* **1992**, *97*, 179.

(34) Dann, S. E.; Weller, M. T. *J. Solid State Chem.* **1995**, *115*, 499.

(35) Nguyen, N.; Er-Rakho, L.; Michel, C.; Choisnet, J.; Raveau, B. *Mater. Res. Bull.* **1980**, *15*, 891.

(36) Kinoshita, K.; Shibata, H.; Yamada, T. *Physica C* **1991**, *176*, 433.

(37) Cava, R. J.; Santoro, A.; Krajewski, J. J.; Fleming, R. M.; Waszczak, J. V.; Jr., W. F. P.; Marsh, P. *Physica C* **1990**, *172*, 138.

(38) Gregory, D. H.; Weller, M. T.; Rao, C. V. N.; Currie, D. B. *Mater. Res. Bull.* **1992**, *27*, 1309.

(39) Adachi, S.; Sakurai, T.; Yaegashi, Y.; Yamauchi, H.; Tanaka, S. *Physica C* **1992**, *192*, 351.

(40) Takano, Y.; Isobe, M.; Ami, T.; Suzuki, M.; Tanaka, M.; Noro, S.; Yamada, T. *Mater. Res. Bull.* **1995**, *30(2)*, 169.

(41) Tan, Z. Q.; Heald, S. M.; Cheong, S.-W.; Hwang, H. Y.; Cooper, A. S.; Budnick, J. I. *Physica C* **1991**, *184*, 229.

(42) Lightfoot, P.; Pei, S.; Jorgensen, J. D.; Tang, X.-X.; Manthiram, A.; Goodenough, J. B. *Physica C* **1990**, *169*, 464.

(43) Izumi, F.; Takayama-Muromachi, E.; Nakai, Y.; Asano, H. *Physica C* **1989**, *157*, 89.

(44) Salvador, P. A.; Mason, T. O.; Hagerman, M. E.; Poeppelmeier, K. R.; *Chemistry of Advanced Materials: A New Discipline*, Interrante, L. V., Hampden-Smith, M., Eds.; VCH: New York, in press.

$\text{LaLnBa}_2\text{Cu}_2\text{Ti}_2\text{O}_{11}$ (Ln = Y, Er, Tm) the B-cations order into individual $\text{CuO}_{4/2}$ and $\text{TiO}_{4/2}$ planes to create an 8-coordinate A site which is preferentially occupied by the smaller Ln cation.⁹ The layered, ordered quadruple perovskite structure is destabilized when the largest lanthanide, La, is required to occupy the lower 8-coordinate site between the CuO_2 sheets. Thus, the ordering of the B–O framework polyhedra can be influenced by the coordination needs of the supporting A cations. Yttrium selectively occupies the 8-coordinate site in $\text{LaYSrCu}_2\text{O}_6$, an oxygen-deficient Ruddlesden–Popper phase, which suggests that A-cation substitutions in $\text{LaSr}_2\text{CuTiO}_{6.5}$ will yield new mixed-copper titanates. Studies are currently underway to investigate how smaller lanthanide substitutions for lanthanum and calcium substitution for strontium will influence cation and oxygen vacancy ordering.

Conclusions

The potential for the synthesis of novel copper titanates has been demonstrated in $\text{LaSr}_2\text{CuTiO}_{6.5}$, an oxygen-deficient $n = 2$ Ruddlesden–Popper phase. The

synthesis was motivated by an interest in preparing an intergrowth structure of $\text{Sr}_3\text{Ti}_2\text{O}_7$ and $\text{La}_2\text{SrCu}_2\text{O}_6$, in which copper and titanium order over distinct $\text{BO}_{4/2}$ nets. The copper and titanium of $\text{LaSr}_2\text{CuTiO}_{6.5}$ were found to be disordered over a single site by both X-ray diffraction and electron microscopy. Owing to the similarity of the crystal chemistry and internal architecture between $\text{LaSr}_2\text{CuTiO}_{6.5}$ and known layered cuprates, alterations of the A-cation composition has great potential to result in an ordering of both the B cations and oxygen vacancies.

Acknowledgment. This work was supported by the National Science Foundation (Award No. DMR-9120000) through the Science and Technology Center for Superconductivity and the Summer Undergraduate Research Program (G.M.S.). This work also made use of MRL Central Facilities supported by the National Science Foundation, at the Materials Research Center of Northwestern University (Award No. DMR-9120521).

CM960279B